Unlocking the Potential of IEEE 802.11az: A Deep Dive into Ranging Capabilities

Alireza Famili*, Tolga Atalay†, Angelos Stavrou*†
*WayWave Inc, Virginia, USA
†Department of Electrical & Computer Engineering, Virginia Tech, Virginia, USA
afamili@waywave.com, tolgaoa@vt.edu, angelos@vt.edu

***Abstract*—Accurate ranging and localization are crucial for the success of various applications, such as autonomous drones navigating, complex urban landscapes, and immersive augmented and virtual reality experiences (AR/VR) in the Metaverse. While outdoor environments benefit from the precision of Global Positioning System (GPS) technology, indoor settings present unique challenges that demand innovative solutions. IEEE 802.11az, also known as Next Generation Positioning (NGP), is engineered to address these challenges by enhancing indoor ranging and positioning accuracy. This paper delves into the critical factors that influence the ranging effectiveness of IEEE 802.11az technology. Through an extensive simulation campaign, we examine how various elements, including bandwidth, the number of transmit and receive antennas, and other environmental factors, impact the accuracy of indoor ranging. Our findings aim to provide a detailed understanding of the technological and practical considerations essential for optimizing IEEE 802.11az implementations.**

***Index Terms*—IEEE 802.11az, indoor ranging, localization**

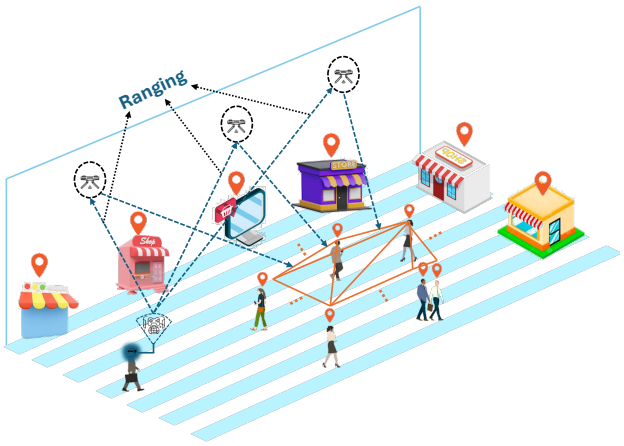

Fig. 1: Indoor ranging between users and Wi-Fi access points

I. Introduction

In today's interconnected world, high-accuracy ranging and localization have become foundational technologies with profound impacts across a wide spectrum of applications. From enabling autonomous vehicles to navigating city streets safely [1]–[3] to facilitating seamless augmented and virtual reality (AR/VR) experiences that blend digital objects with the physical world [4], the precision of location data is paramount. Moreover, in healthcare, accurate indoor tracking systems are critical for asset management and emergency response enhancement, directly influencing patient care quality [5].

While the Global Positioning System (GPS) has revolutionized outdoor navigation, its effectiveness diminishes in indoor environments and in applications requiring ultra-precise localization [6]. To address this, a plethora of technologies such as Ultra-Wideband (UWB) [7], Radio Frequency Identification (RFID) [8], and others have been explored for enhanced positioning capabilities. Among these, cellular positioning [9] and Wireless Fidelity (Wi-Fi) positioning [10] stand out as pioneers that do not necessitate new infrastructure installation and offer more globally accessible location services. While cellular localization has been integral since the first generation of mobile networks, primarily for emergency call services, it demonstrates coarse accuracy [11]. Wi-Fi localization was introduced with IEEE 802.11v, enhancing network efficiency and supporting indoor location-based services.

Both technologies have seen substantial advancements over the years. For instance, the latest developments in millimeter-wave (mmWave) 5G have brought accurate localization to the forefront, achieving ranging precision down to the centimeter. However, cellular technologies face challenges indoors due to signal attenuation and path loss, especially with mmWave frequencies, limiting their effectiveness without additional infrastructure. In contrast, Wi-Fi remains a viable solution for indoor environments. Within the IEEE 802.11 community, commonly referred to as Wi-Fi, a specific project dedicated to directly enhancing localization capabilities is underway, known as Next Generation Positioning (NGP) or IEEE 802.11az.

Figure 1 illustrates a geolocation scenario with users relying on ranging information for indoor localization. In this paper, our focus is to demystify the ranging capabilities of IEEE 802.11az technology through extensive simulation campaigns. 802.11az builds on the advancements of previous Wi-Fi standards to significantly improve indoor positioning accuracy. It introduces High-Efficiency (HE) ranging Physical layer (PHY) Protocol Data Units (PPDUs) in two formats: HE ranging Null Data Packets (NDP) and HE Trigger-Based (TB) ranging NDP, both designed to enhance Time of Arrival (ToA) measurements.

A key feature of the NGP technology is the use of super-resolution techniques, such as Multiple Signal Classification (MUSIC), for precise ToA estimation in multipath environments. This standard supports the use of secure High-Efficiency Long Training Field (HE-LTF) sequences, which can be repeated to further improve ranging accuracy. Our study systematically analyzes how factors like Signal-to-Noise Ratio

979-8-3315-2096-0/25/$31.00 ©2025 IEEE

(SNR), bandwidth, and HE-LTF repetitions affect the precision of these ranging measurements, providing critical insights into the capabilities and limitations of IEEE 802.11az for next-generation indoor localization.

The contributions of our work are as follows:

- We provide a detailed analysis of IEEE 802.11az ranging capabilities through extensive simulations. Our study focuses on understanding how various factors, like bandwidth, SNR, and the number of HE-LTF repetitions, influence the accuracy of ToA measurements.
- We investigate super-resolution techniques, specifically the MUSIC algorithm, for ToA estimation in multipath environments. Our work demonstrates the effectiveness of these techniques in enhancing the precision of ranging measurements in complex indoor settings.
- We evaluate the performance of IEEE 802.11az under different environmental conditions, providing insights into its capabilities and limitations for next-generation indoor localization. Our findings offer valuable guidance for optimizing Wi-Fi-based positioning systems and highlight the potential of 802.11az to deliver sub-meter accuracy in real-world applications.

II. Background & Related Works

There are different localization techniques with unique strengths and limitations. Methods such as Received Signal Strength (RSS) [12]–[14] and fingerprinting [15] are appealing for their simplicity; however, their efficacy is significantly compromised in dynamic environments where real-time changes are not captured. While these approaches are straightforward, they often fall short in precision and adaptability. On the other hand, Angle of Arrival (AoA) measurements offer higher accuracy through angulation but require complex antenna arrays, making the system intricate and challenging to implement [16].

Among the available methods, ranging-based techniques combined with trilateration emerge as the superior choice for demanding applications that necessitate high-accuracy localization [17]. Unlike RSS and fingerprinting, ranging is less susceptible to environmental changes and does not rely on pre-established maps. Furthermore, it avoids the complexities associated with AoA [18] by focusing on the measurement of the time or distance between the transmitter and receiver to pinpoint locations. This method strikes a balance between simplicity and precision, avoiding the major pitfalls of other techniques. For cutting-edge applications, where precision is paramount, trilateration based on accurate ToA and ranging measurements provides the most reliable input data, ensuring robust and precise localization even in challenging settings [19].

Wi-Fi localization began with IEEE 802.11v in 2011, designed to enhance network management by allowing data collection from network-connected devices to support basic location awareness. Although it laid the groundwork, it was IEEE 802.11mc, introduced in 2016, that made significant strides in indoor positioning. This standard, also known as Wi-Fi Fine Timing Measurement (FTM), allowed for precise measurement of signal travel times between devices and access points, achieving location accuracies up to one meter.

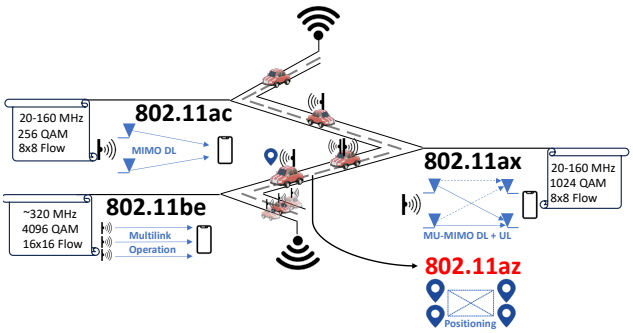

Fig. 2: The recent transition journey from 802.11ac (Wi-Fi 5) to 802.11be (Wi-Fi 7) with the emergence of 802.11az (NGP) in between, specifically designed for advanced positioning

Subsequent Wi-Fi generations, including Wi-Fi 5 (802.11ac) [20], [21] and Wi-Fi 6 (802.11ax) [22]–[24], continued to incorporate and refine these localization capabilities, focusing on improving signal processing and management to support higher densities of devices and applications requiring more precise spatial data. These standards enhanced the accuracy and reliability of existing methods without fundamentally changing the localization approach.

The latest in these series of enhancements is IEEE 802.11az, or NGP, which further improves on the precision introduced by 802.11mc by integrating advanced time and angle measurement techniques [25]. NGP aims to provide sub-meter accuracy essential for cutting-edge applications like augmented reality and detailed asset tracking in complex environments.

III. Fundamentals of IEEE 802.11az Ranging

This section introduces the ranging framework implemented in IEEE 802.11az NGP, aimed at providing users with precise real-time location data in indoor multipath environments. The transition from Wi-Fi 5 (802.11ac) to Wi-Fi 7 (802.11be) is illustrated in Figure 2. Within this journey, the IEEE 802.11az standard introduces a refined approach to Time of Arrival ToA estimations, significantly leveraging the super-resolution capabilities of the MUSIC technique, as detailed in [26].

IEEE 802.11az supports bandwidths up to 160 MHz, introducing two novel High-Efficiency (HE) ranging Physical Layer (PHY) Protocol Data Units (PPDUs): the HE ranging Null Data Packet (NDP) and the HE Trigger-Based (TB) ranging NDP. These PPDUs are designed to enhance ToA measurements, drawing parallels to the HE sounding NDP and HE TB feedback NDP PPDU formats from the 802.11ax standard, which are crucial for their respective localization functions.

Ranging Mechanism: The ranging process involves the transmission of HE ranging NDPs, which facilitate the positioning of users through secure High-Efficiency Long Training Field (HE-LTF) sequences. For single users, the waveform incorporates HE-LTF symbols tailored for individual scenarios, optionally including a secure sequence. Conversely, the multi-user waveform is restricted to secure HE-LTF symbols suitable

Algorithm 1 IEEE 802.11az Ranging Using MUSIC Algorithm

Require: Channel Frequency Response (CFR) data
Ensure: Estimated ToA
1: **Procedure:** MUSIC Ranging
2: Interpolate absent subcarriers in CFR to achieve uniform subcarrier spacing
3: Construct correlation matrix from estimated CFR
4: Apply spatial smoothing to reduce correlation between multipath components
5: Use forward-backward averaging to enhance accuracy of the correlation matrix
6: Treat CFR estimates from different spatial streams as distinct snapshots
7: Incorporate all snapshots into correlation matrix analysis
8: Conduct eigendecomposition of the correlation matrix
9: Separate signal and noise subspaces
10: Identify time-domain delay profile where signal and noise subspaces intersect orthogonally
11: Determine ToA by locating initial peak in the multipath delay profile, assuming Direct Line-of-Sight (DLoS) path

for multiple users. To optimize distance estimation, both waveform types may repeat HE-LTF symbols multiple times. This entire process is visually detailed in Figure 3, with the process step-by-step breakdown in Algorithm 1.

Foundation of MUSIC: The MUSIC algorithm, central to our framework, operates by estimating the power spectrum based on the eigenvalues decomposition of the covariance matrix formed from array sensor data. MUSIC distinguishes between the signal and noise subspaces by identifying the eigenvalues that do not contribute to the signal, thus isolating the directions of arrival of the signal. This super-resolution method is effective in multipath scenarios where it can accurately identify the direct path amidst numerous reflections.

Operational Details: The user begins by transmitting an Uplink (UL) NDP, noting the Time of Departure (ToD) as t_1. The access points (APs) record the ToA as t_2. Subsequently, the APs transmit a Downlink (DL) NDP, marking the ToD as t_3, and the user logs the ToA as t_4. These time stamps facilitate the calculation of the Round Trip Time (RTT), analogous to the FTM used in previous standards, which is crucial for

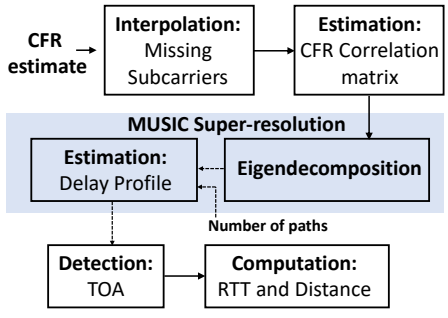

Fig. 3: Overview of the distance ranging process

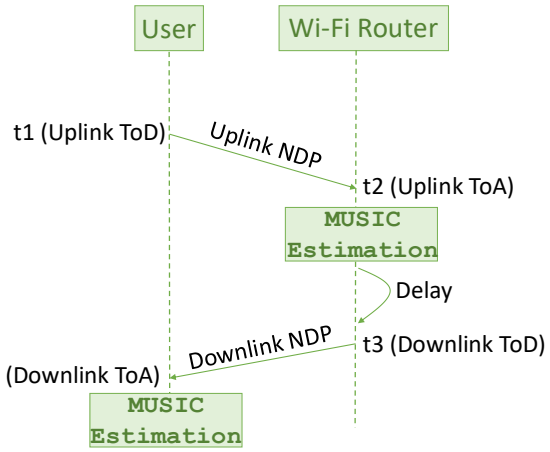

Fig. 4: Measurements of RTT between a user and an AP, analyzed using MUSIC estimation

determining the distance:

$$R_{RTT} = (t_4 - t_1) - (t_3 - t_2). \quad (1)$$

The distance d is computed as $d = \frac{R_{RTT}}{2} \times c$, where c is the speed of light. The steps involved in this procedure are depicted in Figure 4, which visually summarizes the measurement sounding phase between an AP and a user. For a detailed procedural breakdown, refer to Algorithm 2, which outlines the step-by-step method for calculating RTT and distance.

Bandwidth Considerations: The IEEE 802.11 standards, specifically Wi-Fi 5 (802.11ac) and Wi-Fi 6 (802.11ax), technically support a range of bandwidths including 20 MHz, 40 MHz, 80 MHz, and 160 MHz. However, in practical applications, 20 MHz and 40 MHz bandwidths are predominantly utilized due to their sufficient performance and compatibility with a wide range of devices and environments. In contrast, IEEE 802.11az leverages the 160 MHz bandwidth more extensively, capitalizing on its potential to significantly enhance ToA precision in indoor localization scenarios.

Validation through Simulations: To assess the effectiveness of the MUSIC-based ranging method in multipath settings, we focus on the impact of bandwidth expansion in IEEE 802.11az. Figure 5 illustrates the multipath delay profiles obtained using the MUSIC algorithm at different bandwidths, highlighting the

Algorithm 2 Ranging Timestamps and RTT Calculation

Require: Transmission and reception timestamps
Ensure: Distance between user and AP
1: **Procedure:** Calculate RTT
2: User sends Uplink (UL) NDP, logs Time of Departure (ToD) as t_1
3: AP records ToA of UL NDP as t_2
4: AP sends Downlink (DL) NDP, logs ToD as t_3
5: User records ToA of DL NDP as t_4
6: Calculate RTT using: $R_{RTT} = (t_4 - t_1) - (t_3 - t_2)$
7: Calculate distance: $d = \frac{R_{RTT}}{2} \times c$, where c: speed of light

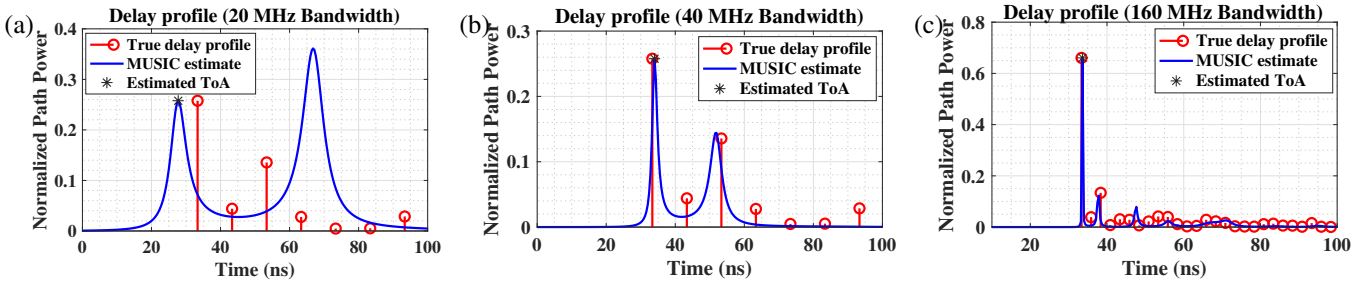

Fig. 5: Illustration of an 802.11 packet's journey through a multipath channel, utilizing the MUSIC super-resolution method to determine the delay profile and ToA across differing bandwidths: (a) 20 MHz; (b) 40 MHz; (c) 160 MHz

performance gains when employing the 160 MHz bandwidth. While previous standards such as Wi-Fi 5 and Wi-Fi 6 commonly utilized narrower bandwidths of 20 MHz and 40 MHz, IEEE 802.11az's predominant use of 160 MHz offers a novel exploration into higher precision ranging. Figure 5 compares the delay profiles from 20 MHz and 40 MHz settings, familiar in earlier Wi-Fi versions, against the 160 MHz setting which is a hallmark of 802.11az. This comparison, showcased in Figures 5(a), 5(b), and 5(c), explicitly demonstrates that increasing the bandwidth enhances the MUSIC algorithm's accuracy in determining the ToA, providing a compelling argument for the adoption of higher bandwidths in complex indoor environments where precise localization is critical.

IV. Comprehensive Ranging Assessment

This section presents the analysis of indoor ranging capabilities facilitated by IEEE 802.11az APs. The simulations critical to our study were performed on a MacBook Pro, which features an Apple M3 MAX CPU and is equipped with 64 GB of RAM. All computational tasks were executed using MATLAB 2024a, utilizing toolboxes designed for NGP indoor positioning with real-life parameter values [27], [28].

The analysis initiates with the user and the NGP AP exchanging ranging measurements. This method is replicated systematically across a spectrum of potential locations within various indoor environments that a user might navigate. Such comprehensive replication allows for a thorough evaluation of our ranging strategy's performance at a multitude of key points throughout the indoor settings.

To ensure a comprehensive and inclusive evaluation, simulations are conducted in a spacious indoor environment measuring $25\ \text{m} \times 25\ \text{m} \times 4\ \text{m}$. The NGP AP is centrally located at $(12.5\ \text{m}, 12.5\ \text{m}, 4\ \text{m})$. The user's potential locations within the space are defined on a grid as follows:

$$x \in \{0\ \text{m},\ 0.5\ \text{m},\ 1\ \text{m},\ \ldots,\ 25\ \text{m}\} \quad (\Delta x = 0.5\,\text{m}),$$
$$y \in \{0\ \text{m},\ 0.5\ \text{m},\ 1\ \text{m},\ \ldots,\ 25\ \text{m}\} \quad (\Delta y = 0.5\,\text{m}),$$
$$z \in \{0\ \text{m},\ 0.5\ \text{m},\ 1\ \text{m},\ \ldots,\ 3\ \text{m}\} \quad (\Delta z = 0.5\,\text{m})$$

Simulations involve generating a ranging NDP, with delays adjusted to reflect distances to the NGP AP from various points within the environment. These adjustments account for both fractional and integer sample shifts to accurately model the signal propagation.

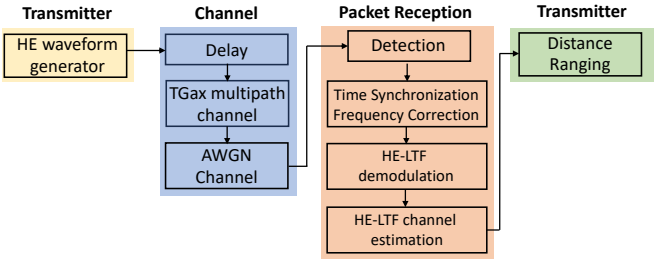

Fig. 6: Simulation procedure for the ranging framework

The detailed sequence of transmission and reception, along with the processing steps for each link between the user and the NGP AP, is depicted in Figure 6. This aids in understanding the measurement exchange process and facilitates accurate distance estimation within our simulated system.

Next, we describe the specific configurations employed in our experiments, focusing on the waveform characteristics exchanged between the user and the NGP AP, as well as the channel setup parameters. Certain parameters are maintained constant across all simulations to ensure consistency, while others are varied to explore their effects on the system performance. This approach allows us to identify optimal settings for the Wi-Fi AP, maximizing the benefits of the IEEE 802.11az standard. All these parameters, both the constant ones and the variables, are detailed in Table I.

Over-the-Air Configuration: The configuration for wave-

TABLE I: Over-the-Air Parameters

Parameters	Values
Carrier Frequency	5 GHz
Bandwidth	(20, 40, 160) MHz
# of TX Antenna	1-3
# of RX Antenna	1-3
# of Space-Time Streams	1-3
Guard Interval	1.6 μsec
Breakpoint Distance	5 m
RMS Delay Spread	15 nanoseconds
Maximum Delay	160 nanoseconds
Rician K-factor	0 dB
Number of Taps	9
Number of Clusters	2

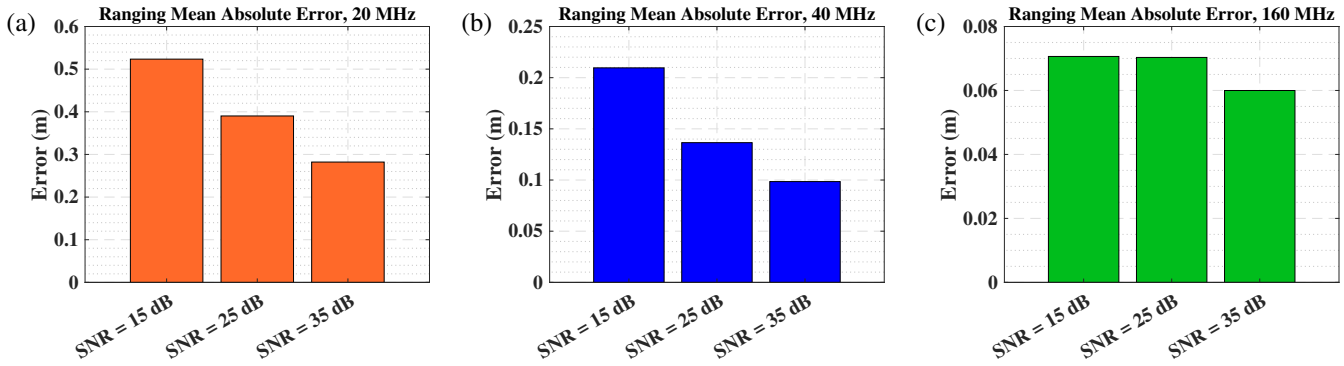

Fig. 7: Mean Absolute Error (MAE) representations for various bandwidths: (a) 20 MHz; (b) 40 MHz; and (c) 160 MHz

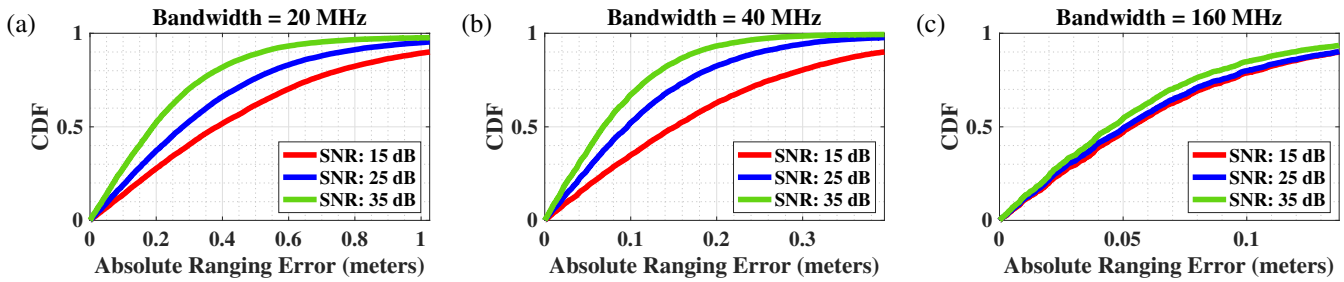

Fig. 8: Illustration of Cumulative Distribution Function (CDF) plots for ranging accuracy across various bandwidths: (a) 20 MHz; (b) 40 MHz; and (c) 160 MHz

form generators at each NGP AP and the user involved several key parameters tailored for this study. The primary channel bandwidth of 160 MHz was chosen in line with IEEE 802.11az specifications. For comparative analysis, this was juxtaposed with 20 MHz and 40 MHz bandwidths, commonly employed in earlier Wi-Fi standards. The setup for both the NGP AP and the user varied from $1-3$ antennas for both transmission and reception, allowing configurations of 1×1 Single Input Single Output (SISO), 2×2 Multiple Input Multiple Output (MIMO), and 3×3 MIMO systems. The experiments utilized $1-3$ space-time streams corresponding to the SISO system and MIMO systems, respectively.

The HE ranging NDP settings were adjusted to require $1-3$ repetitions of the HE-LTF, providing flexibility in signal robustness. A consistent guard interval of 1.6 microseconds was maintained across setups, and the sampling rate was matched to the channel bandwidths of 20, 40, and 160 MHz, to reflect the varied operational conditions. All operations were conducted on a carrier frequency of 5 GHz, optimal for balancing range and interference mitigation. Additionally, the RTT measurement process included a built-in time delay of 16 milliseconds between the UL NDP ToA and the DL NDP ToD, crucial for timing accuracy in the ranging calculations.

Channel Configuration: For the channel setting, we utilized a MATLAB system object to simulate two distinct types of channels. The first channel type is characterized by a predominant DLoS path, which is the strongest among all available paths. This configuration is ideal for evaluating the system's performance in optimal conditions where the direct signal path is clear and unobstructed. The second channel type incorporates a DLoS path that, while still present, is not the most prominent among the paths. This scenario is tailored to assess the system's robustness and accuracy in more complex environments where multiple paths, including reflections and non-line-of-sight components, might affect the signal's integrity and timing measurements.

Evaluation Analysis: Simulations are conducted to evaluate the ranging capabilities at every potential location within the designated area. Each location involves multiple packet exchanges in both uplink and downlink modes between the NGP AP and the user. The first step in our analysis involves calculating the ranging errors at each point under varying channel conditions and noise profiles. All noise profiles are modeled using Additive White Gaussian Noise (AWGN) with different power densities to reflect realistic environmental interferences.

The measured distances between the NGP AP and the user are then rigorously compared with their actual known distances. This core phase of our simulation is essential for estimating the distances from the NGP AP to the user accurately. By analyzing the discrepancies between the measured and actual distances, we can assess the precision and reliability of our ranging methods under varied operational conditions.

Figure 7 illustrates the Mean Absolute Error (MAE) for ranging under various bandwidths. The results are derived from simulations using a 2×2 MIMO system with two space-time streams. The channel parameters were designed to mirror real-

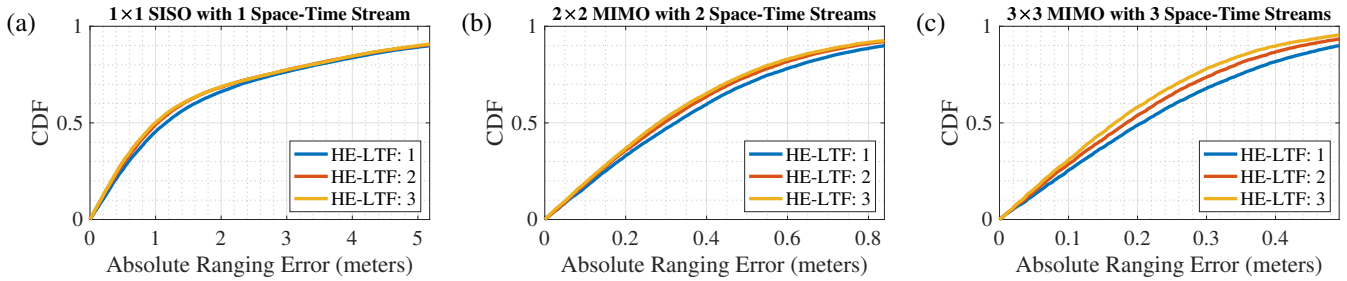

Fig. 9: Illustration of CDF plots for ranging accuracy across various transmit/receive antenna configurations and number of HE-LTF repetition: (a) 1×1 SISO system with one space-time stream; (b) 2×2 MIMO system with two space-time streams; and (c) 3×3 MIMO system with three space-time streams

life conditions of an indoor multipath fading environment. The MAE is computed as the average of the absolute differences between the estimated distances and the actual distances from each point in the area of interest to the NGP AP.

Figures 7(a) and 7(b) showcase the MAE results for the 20 MHz and 40 MHz bandwidths, respectively, which are the most commonly used in Wi-Fi 5 and Wi-Fi 6 for ranging and localization. These serve as benchmarks for our analysis, in contrast to Figure 7(c), which presents results using the 160 MHz bandwidth—predominantly employed in IEEE 802.11az for advanced ranging and localization tasks. Each graph displays the MAE across three different SNRs in the room, from 15 dB to 35 dB. As indicated by the data, higher SNR levels are associated with lower MAE, corroborating the expected inverse relationship between noise levels and measurement accuracy. Furthermore, the data illustrates that the extended bandwidth available in IEEE 802.11az technology substantially enhances ranging accuracy. This improvement is attributed to better multipath resolvability and more accurate ToA detection, underpinning the technological advancements in IEEE 802.11az over its predecessors.

In Figure 8, we illustrate the Cumulative Distribution Function (CDF) for ranging accuracy as it varies across different SNR values and bandwidth settings. Mirroring the approach in Figure 7, we use the 20 MHz and 40 MHz bandwidths in Figures 8(a) and 8(b) as benchmarks for comparison. The CDF for our main proposal, which employs a 160 MHz bandwidth, is showcased in Figure 8(c). Within each figure, the CDF of ranging accuracy for various SNR values is plotted, spanning from 15 dB to 35 dB.

The patterns noted in Figure 7 regarding the impact of SNR and bandwidth on ranging accuracy are similarly reflected in these CDF plots. This consistency confirms that higher SNR values and larger bandwidths contribute to reduced ranging errors. These results highlight the effectiveness of the IEEE 802.11az standard in enhancing ranging accuracy through improved signal processing and bandwidth utilization.

In addition to SNR and bandwidth, our experiments have identified several other parameters critical to the ranging performance in IEEE 802.11az systems, including HE-LTF repetitions, the number of spatial streams, and the number of transmit and receive antennas. Figure 9 provides a detailed summary of the impacts these parameters have on ranging accuracy. Specifically, it illustrates the effects of varying the number of transmit and receive antennas, the number of space-time streams, and the number of HE-LTF repetitions.

For a granular analysis, Figures 9(a), 9(b), and 9(c) display the results for different system configurations: a 1×1 SISO system with one space-time stream, a 2×2 MIMO system with two space-time streams, and a 3×3 MIMO system with three space-time streams, respectively. Each figure explores the influence of increasing HE-LTF repetitions from one to three, assessing their effect on ranging accuracy.

To generate these figures, we utilized the same parameters as previously established for the location of the NGP AP and the grid for the user locations. We conducted the simulations using the same multipath fading channel suited for complex indoor settings, consistent with our earlier tests. The simulations were run with a fixed SNR of 25 dB and a bandwidth of 20 MHz, which allowed us to isolate the effects of other variables under study. Although the predominant bandwidth in IEEE 802.11az is 160 MHz, we conducted these specific simulations at a 20 MHz bandwidth. This decision was made to focus on the influence of antenna configurations, spatial streams, and HE-LTF repetitions without the overarching influence of bandwidth on the outcomes. Using a fixed SNR of 25 dB and a narrower bandwidth, we facilitated faster simulation speeds. While we use a lower bandwidth and SNR for these tests, it is evident from previous results shown in Figures 7 and 8 that higher bandwidths and SNRs would enhance the accuracy of the ranging outcomes. This point underscores that the improvements observed with higher antenna counts, more spatial streams, and increased HE-LTF repetitions would be even more pronounced under higher bandwidth and SNR conditions.

Figure 9 clearly shows that ranging errors decrease with an increase in HE-LTF repetitions, attributed to the noise reduction in the CFR through the averaging of multiple CFR estimates. Furthermore, the results show that higher-order MIMO configurations lead to improved ranging accuracy, which is a result of more CFR snapshots being available from the different spatial streams. These additional snapshots enhance the correlation matrix estimate, facilitating more precise ToA and distance estimations. Moreover, we can see that enhancements in MIMO configurations reduce ranging errors, attributed to the genera-

tion of more CFR snapshots from the available spatial streams. This leads to a more accurate correlation matrix, improving ToA and distance estimations.

V. Conclusion

We conducted a comprehensive analysis of the ranging capabilities of IEEE 802.11az in indoor environments. Our methodology included the development of a detailed test scenario within a large indoor space, where we fixed an NGP AP and assessed the ranging performance across the entire designated environment. We simulated interactions based on real-world parameters reflective of an indoor multipath fading channel. The results from our experiments highlight the significant influence of bandwidth on ranging accuracy; specifically, we found that larger bandwidths lead to higher accuracy. Additionally, the implementation of MIMO systems, featuring multiple transmit and receive antennas along with several space-time streams, was shown to substantially enhance the ranging accuracy in comparison to SISO systems with only one space-time stream. Moreover, our findings demonstrate that an increase in HE-LTF repetitions contributes to a decrease in ranging errors. This improvement is attributed to the effective reduction of noise in the CFR through the averaging of multiple CFR estimates.

References

[1] B. Yang, E. Yang, L. Yu, and C. Niu, "Ultrasonic- and IMU-based high-precision UAV localization for the low-cost autonomous inspection in oil and gas pressure vessels," *IEEE Transactions on Industrial Informatics*, vol. 19, no. 10, pp. 10 523–10 534, 2023.

[2] Y. Sun, W. Wang, L. Mottola, J. Zhang, R. Wang, and Y. He, "Indoor drone localization and tracking based on acoustic inertial measurement," *IEEE Transactions on Mobile Computing*, vol. 23, pp. 7537–7551, 2024.

[3] A. Famili, A. Stavrou, H. Wang, and J.-M. J. Park, "PILOT: high-precision indoor localization for autonomous drones," *IEEE Transactions on Vehicular Technology*, pp. 1–15, 2022.

[4] H. Zhang, S. Mao, D. Niyato, and Z. Han, "Location-dependent augmented reality services in wireless edge-enabled metaverse systems," *IEEE Open Journal of the Communications Society*, pp. 171–183, 2023.

[5] L. Bibbò, R. Carotenuto, and F. Della Corte, "An overview of indoor localization system for human activity recognition (har) in healthcare," *Sensors*, vol. 22, no. 21, 2022. [Online]. Available: https://www.mdpi.com/1424-8220/22/21/8119

[6] A. Famili and J.-M. J. Park, "ROLATIN: robust localization and tracking for indoor navigation of drones," in *2020 IEEE Wireless Communications and Networking Conference (WCNC) (IEEE WCNC 2020)*, 2020.

[7] L. Barbieri, M. Brambilla, A. Trabattoni, S. Mervic, and M. Nicoli, "UWB localization in a smart factory: Augmentation methods and experimental assessment," *IEEE Transactions on Instrumentation and Measurement*, vol. 70, pp. 1–18, 2021.

[8] B. Liang, P. Wang, R. Zhao, H. Guo, P. Zhang, J. Guo, S. Zhu, H. H. Liu, X. Zhang, and C. Xu, "RF-Chord: Towards deployable RFID localization system for logistic networks," in *20th USENIX Symposium on Networked Systems Design and Implementation (NSDI 23)*. Boston, MA: USENIX Association, Apr. 2023, pp. 1783–1799. [Online]. Available: https://www.usenix.org/conference/nsdi23/presentation/liang-bo

[9] A. Famili, T. O. Atalay, A. Stavrou, H. Wang, and J.-M. Park, "OFDRA: Optimal femtocell deployment for accurate indoor positioning of RIS-mounted AVs," *IEEE Journal on Selected Areas in Communications*, vol. 41, no. 12, pp. 3783–3798, 2023.

[10] S. Yang, D. Zhang, R. Song, P. Yin, and Y. Chen, "Multiple WiFi access points co-localization through joint AoA estimation," *IEEE Transactions on Mobile Computing*, vol. 23, no. 2, pp. 1488–1502, 2024.

[11] A. Famili, M. Foruhandeh, T. Atalay, A. Stavrou, and H. Wang, "GPS spoofing detection by leveraging 5G positioning capabilities," in *2022 IEEE Latin-American Conference on Communications*, 2022, pp. 1–6.

[12] A. Aubry, P. Babu, A. De Maio, G. Fatima, and N. Sahu, "A robust framework to design optimal sensor locations for TOA or RSS source localization techniques," *IEEE Transactions on Signal Processing*, vol. 71, pp. 1293–1306, 2023.

[13] G. Guo, R. Chen, X. Niu, K. Yan, S. Xu, and L. Chen, "Factor graph framework for smartphone indoor localization: Integrating data-driven PDR and Wi-Fi RTT/RSS ranging," *IEEE Sensors Journal*, vol. 23, no. 11, pp. 12 346–12 354, 2023.

[14] Z. Xu, B. Huang, B. Jia, and G. Mao, "Enhancing wifi fingerprinting localization through a co-teaching approach using crowdsourced sequential RSS and IMU data," *IEEE Internet of Things Journal*, vol. 11, no. 2, pp. 3550–3562, 2024.

[15] A. Famili, V. Slyusar, Y. H. Lee, and A. Stavrou, "Vehicular teamwork for better positioning," in *2023 IEEE International Conference on Systems, Man, and Cybernetics (SMC)*, 2023, pp. 3507–3513.

[16] X. Kang, D. Wang, Y. Shao, M. Ma, and T. Zhang, "An efficient hybrid multi-station TDOA and single-station AOA localization method," *IEEE Transactions on Wireless Communications*, vol. 22, pp. 5657–5670, 2023.

[17] A. Famili, A. Stavrou, H. Wang, and J.-M. Park, "iDROP: Robust localization for indoor navigation of drones with optimized beacon placement," *IEEE Internet of Things Journal*, vol. 10, no. 16, pp. 14 226–14 238, 2023.

[18] Y. Zou, L. Wu, J. Fan, and H. Liu, "A convergent iteration method for 3-D AOA localization," *IEEE Transactions on Vehicular Technology*, vol. 72, no. 6, pp. 8267–8271, 2023.

[19] G. Himona, A. Famili, A. Stavrou, V. Kovanis, and Y. Kominis, "Isochrons in tunable photonic oscillators and applications in precise positioning," in *Physics and Simulation of Optoelectronic Devices XXXI*, vol. 12415. SPIE, 2023, pp. 82–86.

[20] A. B. Pizarro, J. P. Beltrán, M. Cominelli, F. Gringoli, and J. Widmer, "Accurate ubiquitous localization with off-the-shelf IEEE 802.11ac devices," in *Proceedings of the 19th Annual International Conference on Mobile Systems, Applications, and Services*, ser. MobiSys '21. New York, NY, USA: Association for Computing Machinery, 2021, p. 241–254. [Online]. Available: https://doi.org/10.1145/3458864.3468850

[21] F. Bellili, S. B. Amor, S. Affes, and A. Ghrayeb, "Maximum likelihood joint angle and delay estimation from multipath and multicarrier transmissions with application to indoor localization over IEEE 802.11ac radio," *IEEE Transactions on Mobile Computing*, vol. 18, pp. 1116–1132, 2019.

[22] T. O. Atalay, A. Famili, D. Stojadinovic, and A. Stavrou, "Demystifying 5G traffic patterns with an indoor RAN measurement campaign," in *GLOBECOM 2023 - 2023 IEEE Global Communications Conference*, 2023, pp. 1185–1190.

[23] E. Khorov, A. Kiryanov, A. Lyakhov, and G. Bianchi, "A tutorial on IEEE 802.11ax high efficiency WLANs," *IEEE Communications Surveys & Tutorials*, vol. 21, no. 1, pp. 197–216, 2019.

[24] F. Gringoli, M. Cominelli, A. Blanco, and J. Widmer, "AX-CSI: enabling CSI extraction on commercial 802.11ax Wi-Fi platforms," in *Proceedings of the 15th ACM Workshop on Wireless Network Testbeds, Experimental Evaluation & CHaracterization*, ser. WiNTECH '21. New York, NY, USA: Association for Computing Machinery, 2021, p. 46–53. [Online]. Available: https://doi.org/10.1145/3477086.3480833

[25] A. Famili, T. Atalay, A. Stavrou, and H. Wang, "Wi-Six: Precise positioning in the Metaverse via optimal Wi-Fi router deployment in 6G networks," in *2023 IEEE International Conference on Metaverse Computing, Networking and Applications (MetaCom)*, 2023, pp. 17–24.

[26] X. Li and K. Pahlavan, "Super-resolution TOA estimation with diversity for indoor geolocation," *IEEE Transactions on Wireless Communications*, vol. 3, no. 1, pp. 224–234, 2004.

[27] "802.11az Positioning Using Super-Resolution Time of Arrival Estimation - MATLAB & Simulink," https://www.mathworks.com/help/wlan/ug/802-11az-indoor-positioning-using-super-resolution-time-of-arrival-estimation.html, 2020, (Accessed on 08/08/2023).

[28] I. C. S. L. S. Committee, "IEEE Standard for Information technology-Telecommunications and information exchange between systems-Local and metropolitan area networks-Specific requirements Part 11: Wireless LAN Medium Access Control (MAC) and Physical Layer (PHY) Specifications," *IEEE Std* 802.11^{TM}, 2019.